

Source parameters estimation of the 1980 Bajhang Earthquake, far western Nepal

K.N. Khanal

Central Department of Physics
Tribhuvan University, Kathmandu, Nepal

ABSTRACT

The Bajhang earthquake of 1980 is one of the moderate magnitude earthquakes in the Himalaya that has been investigated by many researchers. The methods used by them for determining source parameters vary from the use of the first motion data to the waveform modeling. The ambiguity in focal mechanisms determined by different processes has been resolved by comparing the synthetic seismograms generated using wave number integration technique with those observed at the Global Digital Seismograph Networks (GDSN). The earthquake source parameters determined are found to be as follows: Dip=26°, Strike=290°, Rake=90°, Depth of focus=20±5 km and source time function=7 (2,3,2) seconds.

INTRODUCTION

The Bajhang earthquake of 1980 has drawn attention of many researchers in the world (Ni and Barazangi, 1984; Singh, 1985; Sipkin, 1987; Choy and Engdahl, 1987; Lyon-Caen and Molnar, 1989). The event having its body wave magnitude 6.1 and surface wave magnitude 6.5 had affected an area of 12000 km² (Singh, 1985). The tectonics of the epicentre region (Fig. 1) has been explored by many investigators (e.g., Seeber et al., 1981; Khattri and Tyagi, 1983; Baranowski et al., 1984; Ni, 1989; Molnar, 1990; Khattri et al., 1993; Yu et al., 1995).

One of the reliable methods used in order to estimate the earthquake source parameters is the waveform modeling that requires the generation of synthetic seismograms with the appropriate earth model. Various approaches are taken in order to generate such seismograms. In this method, the wave number or the frequency integral is evaluated first (Chapman, 1978). If the wavenumber integral is evaluated first leaving the frequency integral, it is known as the spectral method (Langston and Helmberger, 1975; Hermann, 1978; Mueller, 1985). If the frequency is integrated, first it is called slowness method (Burdick and Orcutt, 1979). In this study, the wave number integration method has been used to generate synthetic seismograms of the long

period P waves. High quality digital observed seismograms from the Global Digital Seismograph Networks are used in this investigation.

THEORY INVOLVED

As the seismogram is the net effect of source, medium and instrument systems, the synthetic seismogram is expressed as the convolutional output of the responses of all these systems:

$$r(t) = s(t) * s^c(t) * r^c(t) * i(t)$$

where, $s(t)$ describe the seismic radiation at the focal sphere,
 $s^c(t)$ and $r^c(t)$ are the impulse responses in the source and in the receiver region respectively,
 $q(t)$ is the Q factor in time domain
 $i(t)$ is the instrumental response and * denotes convolution

METHODOLOGY

The source crust response is estimated according to Hudson (1969a,b). The source crust is composed of horizontally isotropic, homogeneous layers. Each layer is characterized by the P and the S wave velocities, the density and the thickness. The source

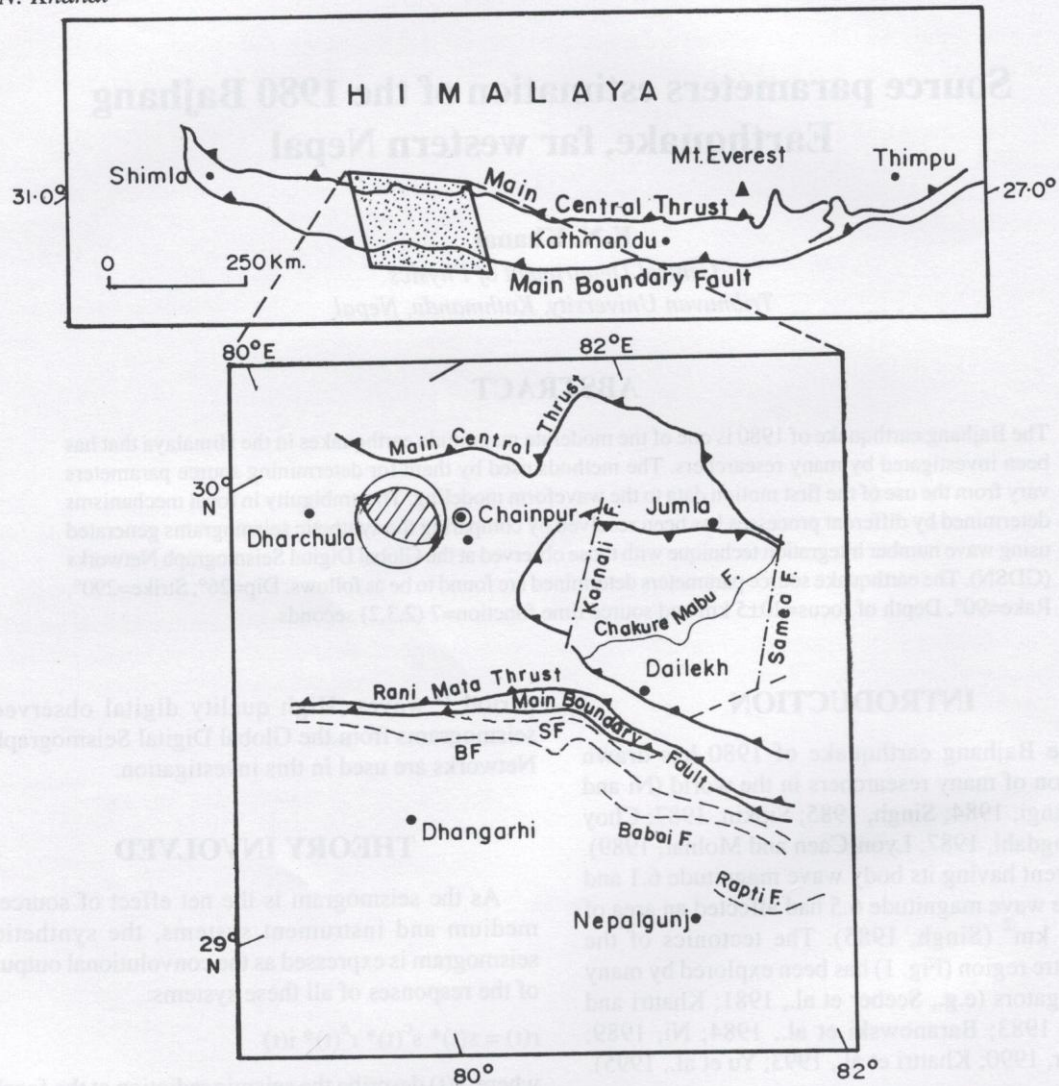


Fig. 1: Tectonics of the epicentral region of the earthquake. BF: Bheri Fault, SF: Surkhet Fault (after Department of Mines and Geology).

is supposed to be at one of the layers. The boundary conditions of stress motion vector have been applied to evaluate the source crust response. The mantle response is evaluated by taking account of the quality factor Q that varies as $e^{-w/Q}$, where w is the angular velocity, t is the travel time and Q is the quality factor that is related with inverse of the attenuation. The Q value for the P waves is used as given by Langston and Helmberger (1975). The receiver crust transfer function is estimated by propagator matrix method of Haskell (1953). The appropriate transfer function of the instrument system is used.

The earthquake source is represented by a point dislocation specified by the fault angles, the strength, the depth of focus and the source time function. In this study, moment is used to specify the strength and is treated as the multiplicative factor. The fault plane angles, i.e., dip, strike and rake have been estimated by trial and error procedure. The initial estimate is done using the values obtained by other investigators. At the beginning, the source time function is estimated from the empirical values of the dimension of the source according to Kasahara, 1981 (Table 1).

Source parameters estimation of the 1980 Bajhang Earthquake, far western Nepal

Table 1: Earthquake hypocentral parameters and magnitudes

Date	Origin Time	Latitude °N	Longitude °E	Body wave magnitude (mb)	Surface wave magnitude (Ms)	Depth H(EDR)
1980:7:29	14:58:40.8	29.598	81.092	6.1	6.5	18

Source: Earthquake data reports of United States Geological Survey

The observed seismograms used in this study are those recorded at seven stations (Fig. 2): GUMO (Guam, Merina Island), NWAO (Narogen, Australia), GRFO (Grafenberg, Germany), TATO (Taipei), CTAO (Charter Tower, Australia), MAJO (Matsushire, Japan) and KONO (Kongsberg, Finland). The station parameters that include the location of epicenter and the azimuth (or back azimuth) are estimated assuming a symmetric spherical earth (Richter, 1958). These parameters are presented in Table 2.

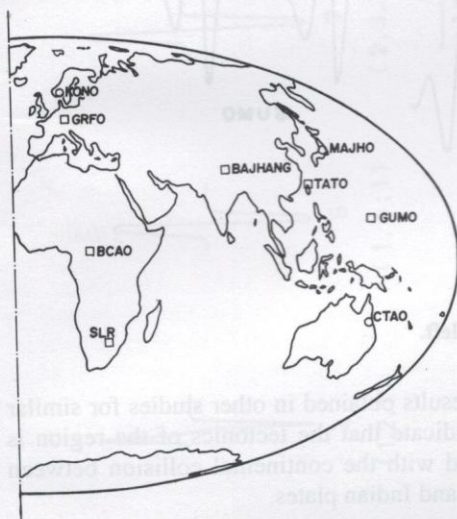


Fig. 2: Various digital stations used for the study.

Table 2: Stations parameters

Station	Epicentral Distance, Degree	Azimuth, Degree	Back Azimuth, Degree	Take Off Angle, Degree	Phase Velocity, Km/sec
GUMO	60.69	90.51	296.55	24.5	14.5
NWAO	71.29	148.48	327.21	21.7	16.2
GRFO	55.24	312.32	96.38	26.0	13.7
TATO	92.56	286.61	31.4	11.5	
CTAO	80.01	120.08	306.72	19.2	18.2
MAJO	47.67	65.87	260.99	28.1	12.7
KONO	55.55	324.48	90.79	25.9	13.7

Among the various velocity models (Barazangi and Ni, 1982; Ni and Barazangi, 1983; Hirn et al., 1984; Chander et al., 1986) used on trial basis showed the model of Hirn et al., 1984 produced comparatively better result. The model is given in Table 3.

Table 3: Velocity model of the (source crust)

Vp (km/s)	Vs (km/s)	Density (gm/cc)	Thickness of layers(km)
6.0	3.45	2.7	20
6.4	3.75	2.9	35
8.0	4.82	3.3	—

RESULT

The location of the earthquake epicentre along with the tectonics of the region is shown in Fig. 1. From the digital observed seismograms (Fig. 3) the source parameters are estimated as strike=290°, dip=26°, rake=90°, duration of source time function =2,3,2 (7) seconds and depth of focus=20±5 km. Fig. 4a shows the total duration of the rupture of seconds fits the rupture of the earthquake. Fig. 4b shows a linear dependence between duration of source time function and the period of the waves.

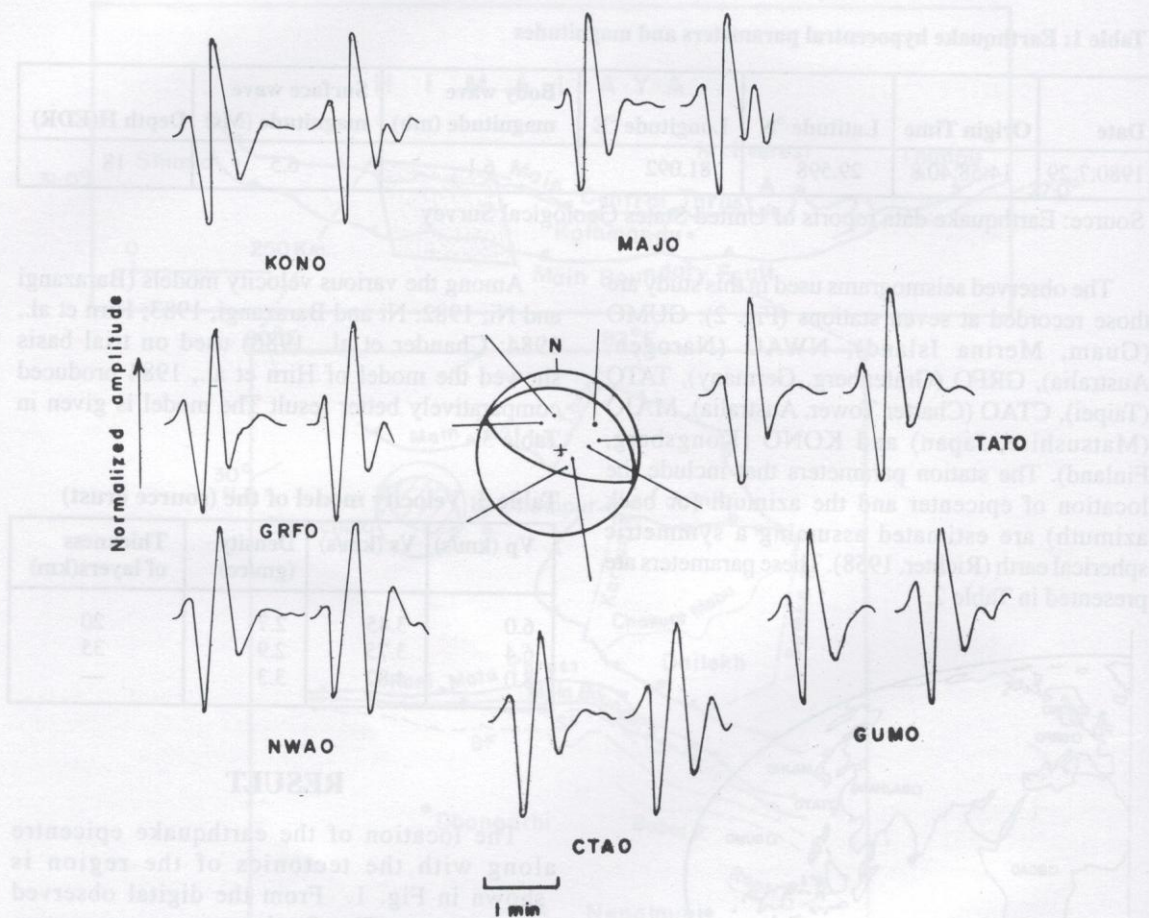


Fig. 3: Synthetic and observed seismograms. Synthetics are on the left.

DISCUSSION AND CONCLUSIONS

A comparison between synthetic and observed seismograms (Fig. 3) shows that there are some differences in the period and first peak to peak amplitude of the waves which may be due to various factors including the very simple receiver crust model and the inadequate path effects taken into consideration.

The shape of the seismograms are also dependent on fault plane parameters. The angles specifying the earthquake source are resolvable only up to an angle of ± 5 in this study. The period of the waves match good indicating that the duration of source time function taken into account is appropriate. Although the tectonics of the region cannot be explained in terms of the fault plane solution of a single event

but the results obtained in other studies for similar events indicate that the tectonics of the region is associated with the continental collision between Eurasian and Indian plates.

In this study, the depth of focus has not been resolved properly. Choy and Engdhal (1987) treat it as a complex event and estimate the depth of focus equal to 27 km. Sipkin (1987) estimates only 17 km, whereas Ni and Barazangi (1984) estimates the depth to be only 15 km. Earthquake Data Report reports the depth of the event as 17 km. On the other hand, International Seismological Summary has estimated 23 km whereas from this study the depth has been constrained to be at 20 ± 5 km. It is believed that the estimation of 20 km made in this study is not away from the real value (Baranowski et al., 1984).

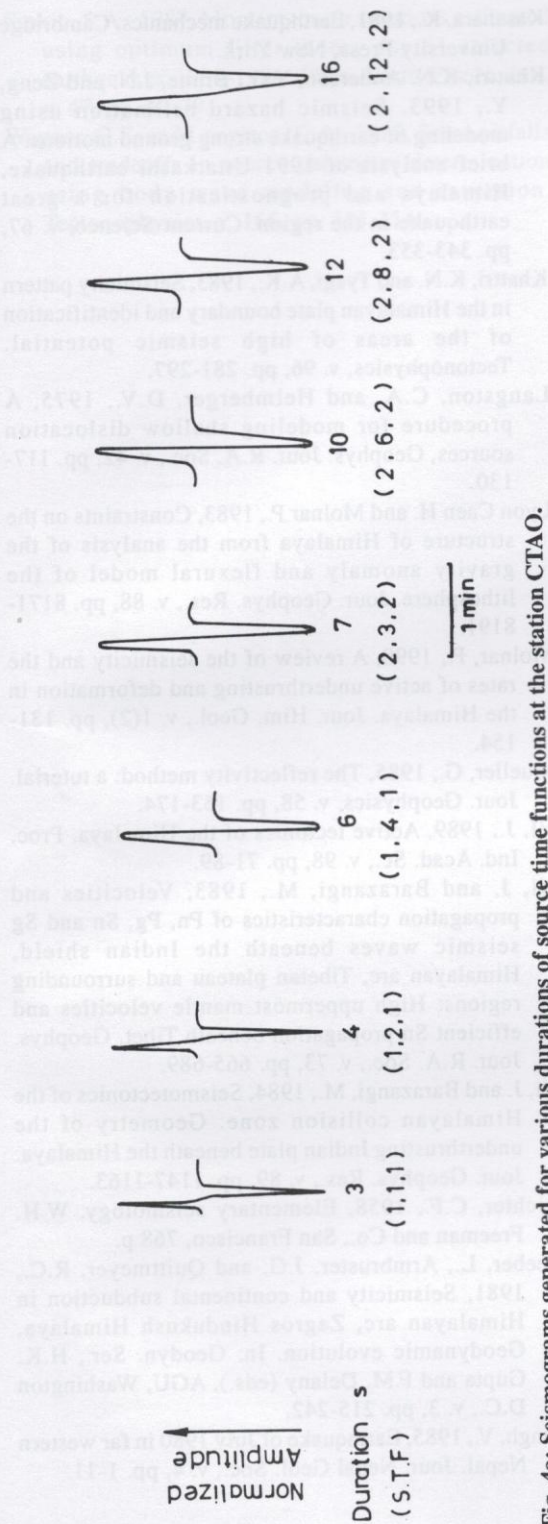


Fig. 4a: Seismograms generated for various durations of source time functions at the station CTAO.

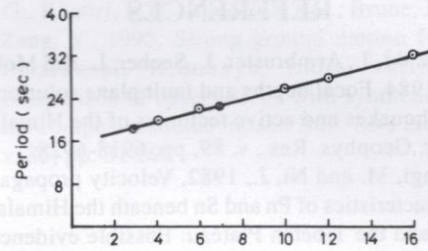


Fig. 4b: Relation between the duration of source time function and the periods of the waves.

One of the significant differences that occurs in the body wave modeling is in between the depth of focus and the source time function (e.g., Christensen and Ruff, 1985). In some cases, it is possible to fit observed data using a deep source with a short source time function as well as a shallower source with a longer time function (Wagner and Langston, 1989). This ambiguity can be resolved based on external information. The relationship between the magnitude and the duration of source time function can also be established from the rupture length and the rupture velocity (Kasahara, 1981). In the present investigation, the duration of source time function has been fixed from the curves obtained at various durations (Fig. 4a). For the earthquake of this magnitude, the duration is of about 7 seconds.

Fig. 4b shows the relation between the period of the waves and duration of the source time function. A linear relation has indicated that the longer the duration of source time function i.e., the longer the slip of the fault the longer will be the period of the wave. It is based on the practical experience.

ACKNOWLEDGEMENTS

The author expresses his gratitude to Prof. K.N. Khattri, Emmeritus Scientist and Dr. V.C. Thakur, Director, Wadia Institute of Himalayan Geology for their suggestion and help during this work. He is also thankful to the unknown reviewer. Revision of the work was done when the author visited WIHG under scientific exchange program between RONASt and INSA during October, 1995 to April, 1996.

REFERENCES

- Baranowski, J., Armbruster, J., Seeber, L. and Molnar, P., 1984, Focal depths and fault plane solutions of earthquakes and active tectonics of the Himalaya. *Jour. Geophys. Res.*, v. 89, pp. 6918-6928.
- Barazangi, M. and Ni, J., 1982, Velocity propagation characteristics of Pn and Sn beneath the Himalayan arc and the Tibetan Plateau: Possible evidence of underthrusting of Indian continental lithosphere beneath Tibet. *Geology*, v. 10, pp. 179-1485.
- Burdick, L.J. and Orcutt, J.A., 1979, A comparison of the generalized ray and reflectivity methods of waveform synthesis. *Geophys. Jour. Roy. Astr. Soc.*, v. 58, pp. 261-278.
- Chander, R., Sarkar, I., Khattri, K.N., Gaur, V.K., 1986, Upper crustal compressional wave velocity in the Garhwal Himalaya. *Tectonophysics*, v. 124, pp. 133-140.
- Christensen, D.h. and Ruff, L.J., 1985, Analysis of the trade off between hypocentral depth and source time function. *Bull. Seis. Soc. Am.*, v. 75, pp. 1637-1656.
- Chapman, C.H., 1978, A new method for computing synthetic seismograms. *Geophys. Jour. R.A. Soc.*, v. 54, pp. 481-518.
- Choy, G.L. and Engdahl, E.R., 1987, Analysis of broad band seismograms from selected IASPEI events. *Earth and Planet. Int.*, v. 47, pp. 80-92.
- Fuchs, K. and Mueller, G., 1971, Computation of synthetic seismograms with the reflectivity method and comparison with observations. *Geophys. Jour. R.A. Soc.*, v. 23, pp. 417-433.
- Haskell 1953, The dispersion of surface wave on multilayered media. *Bull. Seis. Soc. Am.*, v. 43, pp. 17-34.
- Herrmann, R.B., 1978, Computer program in earthquake seismology. Report of the Saint Louis University, U.S.A. v. 1.
- Hirn, A., Lapine, J.C., Jobert, G., Sapin, M., Wittlinger, G., Xin, X.Z., Yaun, G.E., Jing, W.X., Wen, T.J., Bai, X.S., Pandey, M.R. and Tater, J., 1984, Crustal structure and variability of the Himalayan border of Tibet. *Nature*, v. 307, pp. 23-25.
- Hudson, J.A., 1969a, A quantitative evaluation of seismic signals at teleseismic distances: I. Radiation from point sources. *Geophys. Jour. R.A. Soc.*, v. 18, pp. 233-249.
- Hudson, J.A., 1969b, A quantitative evaluation of seismic signals at teleseismic distances: II. Body waves and surface waves from extended sources. *Geophys. Jour. R.A. Soc.*, v. 18, pp. 353-370.
- Kasahara, K., 1981, Earthquake mechanics. Cambridge University Press, New York.
- Khattri, K.N. Anderson, Y.G., Brune, J.N. and Zeng, Y., 1993. Seismic hazard estimation using modeling of earthquake strong ground motions: A brief analysis of 1991 Uttarkashi earthquake, Himalaya and prognostication for a great earthquake in the region. *Current Science*, v. 67, pp. 343-353.
- Khattri, K.N. and Tyagi, A.K., 1983, Seismicity pattern in the Himalayan plate boundary and identification of the areas of high seismic potential. *Tectonophysics*, v. 96, pp. 281-297.
- Langston, C.A. and Helmberger, D.V., 1975, A procedure for modeling shallow dislocation sources, *Geophys. Jour. R.A. Soc.*, v. 42, pp. 117-130.
- Lyon Caen H. and Molnar P., 1983, Constraints on the structure of Himalaya from the analysis of the gravity anomaly and flexural model of the lithosphere. *Jour. Geophys. Res.*, v. 88, pp. 8171-8191.
- Molnar, P., 1990, A review of the seismicity and the rates of active underthrusting and deformation in the Himalaya. *Jour. Him. Geol.*, v. 1(2), pp. 131-154.
- Mueller, G., 1985, The reflectivity method: a tutorial. *Jour. Geophysics*, v. 58, pp. 153-174.
- Ni, J., 1989, Active tectonics of the Himalaya. *Proc. Ind. Acad. Sc.*, v. 98, pp. 71-89.
- Ni, J. and Barazangi, M., 1983, Velocities, and propagation characteristics of Pn, Pg, Sn and Sg seismic waves beneath the Indian shield, Himalayan arc, Tibetan plateau and surrounding regions: High uppermost mantle velocities and efficient Sn propagation beneath Tibet. *Geophys. Jour. R.A. Soc.*, v. 73, pp. 665-689.
- Ni, J. and Barazangi, M., 1984, Seismotectonics of the Himalayan collision zone: Geometry of the underthrusting Indian plate beneath the Himalaya. *Jour. Geophys. Res.*, v. 89, pp. 1147-1163.
- Richter, C.F., 1958, Elementary seismology. W.H. Freeman and Co., San Francisco, 768 p.
- Seeber, L., Armbruster, J.G. and Quittmeyer, R.C., 1981, Seismicity and continental subduction in Himalayan arc, Zagros Hindukush Himalaya, Geodynamic evolution. In: *Geodyn. Ser.*, H.K. Gupta and F.M. Delany (eds.), AGU, Washington D.C., v. 3, pp. 215-242.
- Singh, V., 1985, Earthquake of July 1980 in far western Nepal. *Jour. Nepal Geol. Soc.*, v. 4, pp. 1-11.

- Sipkin, S.A., 1987, Moment tensor solutions estimated using optimum filter theory for 51 selected earthquakes 1980-1984. *Phys. Earth Planet. Int.*, v. 47, pp. 67-79.
- Wagner, G.S. and Langston, C.A., 1989, Some pitfalls and tradeoffs in source parameter determination using body wave modeling and inversion. *Tectonophysics*, v. 166, pp. 101-114.
- Yu, G., Khattri, K.N., Anderson, J.G., Brune, J.N. and Zeng, Y., 1995, Strong ground motion from the Uttarkashi, Himalaya, India, earthquake: comparison of observations with synthetics using the composite source model. *Bull. Seis. Soc. Am.*, v. 85, pp. 31-50.

Dr. G. M. Schramm
Geology and Palaeontology, University of Salzburg
Hellbrunnstrasse 34/III, 5020 Salzburg, Austria

ABSTRACT

Within the western flank of the Ganesh Himal in central Nepal, an area of complex landslides lies in the Jarlung area, situated at the southeastern slope of the Anika Khola valley. Slow rotational rockslide in strongly weathered muscovite-quartzite underlaying with muscovite have destabilized the head scarp composed of argillaceous gneiss. It caused rockslides from the main scarp generating big spread-out landslides. The landslide of Jarlung generated a stratified deposit (1980 m³) of matrix-rich breccias with thin fine-grained shear horizons.

The initial event for the biggest gully system in central Nepal was a preferential slant owing to head scarp failure initiated in 1974. The recent processes include three sedimentary deposits and rotational gully system accompanied by excessive rotational and translational slides along the gully margins. The high activity within the Jarlung gully system can be explained by reactivation of the old Jarlung landslide's shear surfaces. The slide grew from an original width of 300 m to 1.2 km at present, covering an area of 2.65 km². The total volumetric loss by 1996 is 1.45×10^7 m³.

The triggering factor for rock slides and rock falls generating big spread-out landslides and debris slides and slope undercutting is seismic events due to extremely high uplift of the Himalayan Geogeny. The strong influence of human activities on slope stability and mass wasting as proposed in the Himalayan *Three-dimensional Deformation Theory* can not be validated.

GEOGRAPHIC FEATURES AND CLIMATE

The study area lies at the southern flank of the Ganesh Himal's main ridge (28°N, 83°E) in the Dhaulagiri district (central Nepal) about 30 km. It is divided by the 4000 m high, N-S running, rocky and sharp-edged ridges Kinpa and Maryang Danda and very deep gorges. The study area is situated in the mid stage between 1400-1500 m (Thaler, 1981), which is most severely hit by the summer monsoon impact, with 3000-4000 mm of precipitation within five and a half months, nearly all the year, even during the winter monsoon, precipitation is very low, only the summer monsoon and exceptional high cyclones bring heavy rainfall (Thompson and Devkota, 1989). The mid stage is subdivided into the cultivated lower mid stage (1400-1500 m) and the wooded higher mid stage (1500-1600 m). The

lower subtropical stage, elevation between 900 and 1500 m, with red colored ferrallitic soil, is not developed in the study area (Thaler, 1981).

GEOLOGIC SETTING

The lithology is dominated by Palaeozoic mica quartzites of the Lower Mulland Formation of La Fort (1975) corresponding to the Kincha Formation of Stocklin (1980), weakly by intercalations of mica schists with discontinuous levels of thick and compact ortho gneiss (Lilien argillaceous gneiss) and small amounts of amphibolite (Fig. 1). The metamorphic grade of the rocks is green schist facies (Parker, 1977).

The tectonic structures were formed by successive deformation stages (Parker, 1977). In the study area, the most important ones are: